

## Transport Barrier Formation by Application of Localized ECH in the LHD

S. Kubo, T. Shimozuma, H. Idei, Y. Yoshimura, T. Notake<sup>1</sup>, M. Sato, K. Ohkubo, T. Watari, K. Narihara, I. Yamada, S. Inagaki, Y. Nagayama, S. Murakami, S. Muto, Y. Takeiri, M. Yokoyama, N. Ohyabu, K. Ida, K. Kawahata, O. Kaneko, A. Komori, T. Mutoh, Y. Nakamura, H. Yamada, T. Akiyama<sup>2</sup>, N. Ashikawa, M. Emoto, H. Funaba, P. Goncharov<sup>3</sup>, M. Goto, K. Ikeda, M. Isobe, H. Kawazome<sup>4</sup>, K. Khlopenkov, T. Kobuchi, A. Kostrioukov, R. Kumazawa, Y. Liang, S. Masuzaki, T. Minami, J. Miyazawa, T. Morisaki, S. Morita, H. Nakanishi, Y. Narushima, K. Nishimura, N. Noda, H. Nozato<sup>5</sup>, S. Ohdachi, Y. Oka, M. Osakabe, T. Ozaki, B. J. Peterson, A. Sagara, T. Saida<sup>3</sup>, K. Saito, S. Sakakibara, R. Sakamoto, M. Sasao, K. Sato, T. Seki, M. Shoji, H. Suzuki, N. Takeuchi<sup>1</sup>, N. Tamura, K. Tanaka, K. Toi, T. Tokuzawa, Y. Torii<sup>1</sup>, K. Tsumori, K.Y. Watanabe, Y. Xu, S. Yamamoto<sup>1</sup>, T. Yamamoto<sup>1</sup>, M. Yoshinuma, K. Itoh, T. Satow, S. Sudo, T. Uda, K. Yamazaki, K. Matsuoka, O. Motojima, Y. Hamada, and M. Fujiwara

National Institute for Fusion Science, Toki, Gifu 509-5292, Japan

<sup>1</sup> Department of Energy Engineering and Science, Nagoya University, 464-8603, Japan

<sup>2</sup> Research Laboratory for Nuclear Reactors, Tokyo Institute of Technology, Tokyo 152-8550, Japan

<sup>3</sup> Department of Fusion Science, School of Mathematical and Physical Science, Graduate University for Advanced Studies, Hayama, 240-0193, Japan

<sup>4</sup> Graduate School of Energy Science, Kyoto University, Uji 611-0011, Japan

<sup>5</sup> Graduate School of Frontier Sciences, The University of Tokyo 113-0033, Japan

e-mail contact of main author: kubo@LHD.nifs.ac.jp

**Abstract.** In the past three years, the LHD [1] has revealed confinement properties as good as those of tokamaks. And achieved beta value of 3.2 % has been attained, satisfying necessary condition to be a candidate for a reactor core [2]. However, a fundamental question remains; whether or not such high performance is maintained in a collisionless regime as the electron temperature gets higher. Indeed, the electron temperature remained below 4 keV for the past 3 years as if it were caught in the vicious dependence that the energy confinement time is proportional to  $T_e^{-7/2}$  as predicted in the neoclassical theory without electric field. This paper reports that a plasma of 10 keV was achieved in the 5th campaign of the LHD, carried out in 2001, resolving such a concern and opening a new regime of extremely low collisionality. This regime of high  $T_e$  has the features of the ITB and is obtained by achieving special experimental conditions.

### 1. Introduction

There was a working hypothesis that a regime of improved confinement is obtained as the heat flux exceeds a certain threshold value [3]. One of the proposed mechanisms of this improvement is the suppression of the turbulent transport by velocity or radial electric field shear. Attaining high electron temperature itself is the result of the improvement of the confinement but also open the way to investigate the improved confinement mechanism in the collisionless regime. Achievement of relatively high electron temperatures has been reported from CHS [4], W7-AS [5] and TJ-II [6], and various explanations have been given for the improved energy confinement. Since the LHD has a higher aspect ratio than the CHS, the LHD has a better orbit of trapped particles, and as the magnetic axis is shifted inward it approaches advanced helical systems in the properties of its drift orbits. Thus, the LHD plays a unique role in understanding the mechanism of the ITB in terms of space potential. The electric field, if it has a key role, would contribute to the reduction of the anomalous parts of  $\chi_e$  rather than to that of the

neoclassical one. The resonance heating on axis became possible in LHD. Almost 1 MW electron cyclotron power is concentrated in the core region of LHD, resulting in the transition from normal to higher confinement in LHD. It is also observed that these transition occurs above a threshold power and this threshold changes as the density. These are similar observation of the ITB in tokamaks and helical systems. In this paper, the attainment of more than 10 keV plasma is reported. This high temperature is attained by triggering the transition by concentrating almost 1 MW power near the central part of the plasma.

In the next section, the plasma attained 10 keV is described with the specific features of the electron cyclotron heating system in LHD. One of the main interests from the view point of confinement barrier, it is of much interest that the presence of foot point of the transport barrier really exist or not. NBI target plasma is used because the foot point is more clear than pure ECH plasma. The ITB (internal transport barrier ) observation on NBI target plasma is described in section 3. Temporal transition and its relation to the temperature gradient is described and implication from these observations are discussed also in section 3.

## 2. Attainment of $T_{e0} = 10$ keV

The central electron temperature of more than 10 keV is achieved in the experimental campaign in 2001. So far, it had not been possible to do efficient heating by ECH on LHD due to the lack of the resonance condition on the axis. The magnetic field at the magnetic axis is increased by shifting the axis inward ( $R=3.5 - 3.6$ ) from the standard position ( $R = 3.75$  m ) to locate the cyclotron layer across the axis. In accordance with this shift in the magnetic axis the steering range of the ECH injection beam was modified [7].

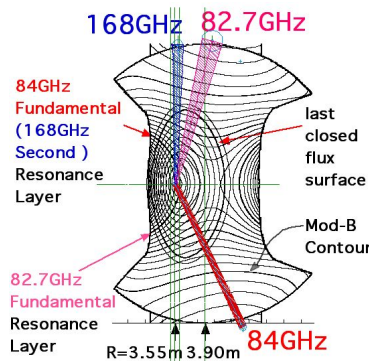


Fig. 1: Flux surfaces and mod-B con-

tours in LHD at vertically elongated cross section. Injected microwave beam profile calculated from ray tracing. Power from horizontal antenna is excluded in this calculation.

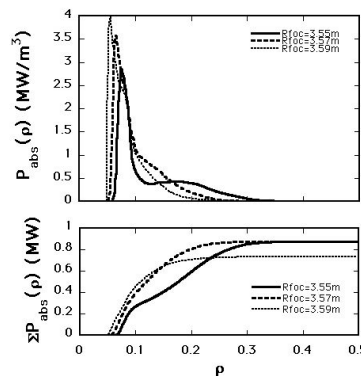


Fig. 2: Expected power deposition Power from horizontal antenna is excluded in this calculation.

rotrons. Each gyrotron delivers 100-400 kW microwave power into the LHD. Figure 1 shows the injection beams, Mod-B contours, and flux surfaces in the vertically elongated poloidal cross section. Two sets of upper beams, one lower beam from a vertical antenna, and two beams from horizontal antennas are used. The magnetic field strength and the configuration are selected to have a power deposition as nearly on axis as possible. The selected magnetic axis is 3.53 m and the toroidally averaged magnetic field strength on the axis is 2.951 T. The expected power deposition profile estimated by ray tracing, including the weakly relativistic effect, indicates that almost all of the injected power from the upper and lower antennas are concentrated within an averaged minor radius of  $\rho \approx 0.2$  as shown in Fig.2, here, three cases of different injection

As a result, ECH beams were concentrated on the shifted axis. For the on axis heating, strongly focussed Gaussian beams at the fundamental and second harmonic resonances are directed to the resonances near the magnetic axis. The microwave sources used are two 84 GHz collector potential depression (CPD)-type gyrotrons, two 82.7 GHz non-CPD gyrotrons, and three 168 GHz CPD gy-

angle is plotted to see the allowances and errors in antenna setting. Lower traces are integrated absorption power. Almost 100% power absorption can be expected in the density, and temperature ranges discussed in this paper, provided that the beams crosses the resonance in the plasma confinement region. Fig.3 shows the evolution of plasma parameters and temperature profiles when the central electron  $T_{e0}$  exceeded 10 keV. The time evolution of the injected total power, the electron density, and the stored energy are shown here for the shot when the highest central electron temperature is recorded in the LHD. Almost 1.2 MW ECH power is concentrated inside  $\rho \approx 0.2$ . The electron density is slightly increasing but stays  $0.5$  to  $0.6 \times 10^{19} \text{m}^{-3}$  in this case.

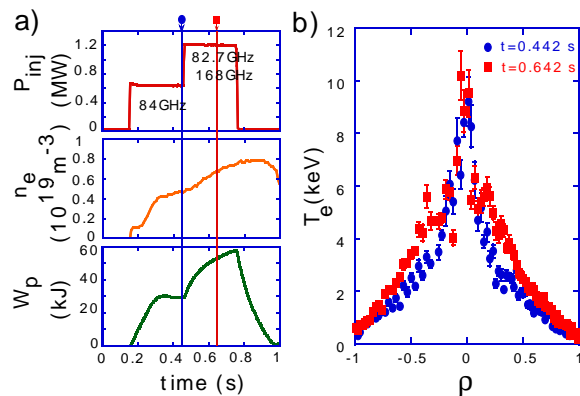


Fig. 3: a) Time evolution of injected ECH power (upper), electron density (middle) and stored energy (bottom). b)  $T_e$  profile measured at each timing indicated by the arrow in a).

The two 84 GHz gyrotrons injected 0.7 MW to produce and heat the plasma. After the density and the stored energy had attained a quasi-steady state, the 168 GHz and 82.7 GHz power are added simultaneously. Although no additional gas puff is supplied, the density keeps increasing slightly. A high power YAG-Thomson scattering system is used at the times indicated by the arrows in Fig.3 a). The profile is already sharp in the phase when only the 84 GHz power is injected. The 82.7 GHz power raises the central electron temperature to more than 10 keV. These high electron temperature modes appear only when the injected power exceeds a certain threshold level, and this threshold level increases with the electron density.

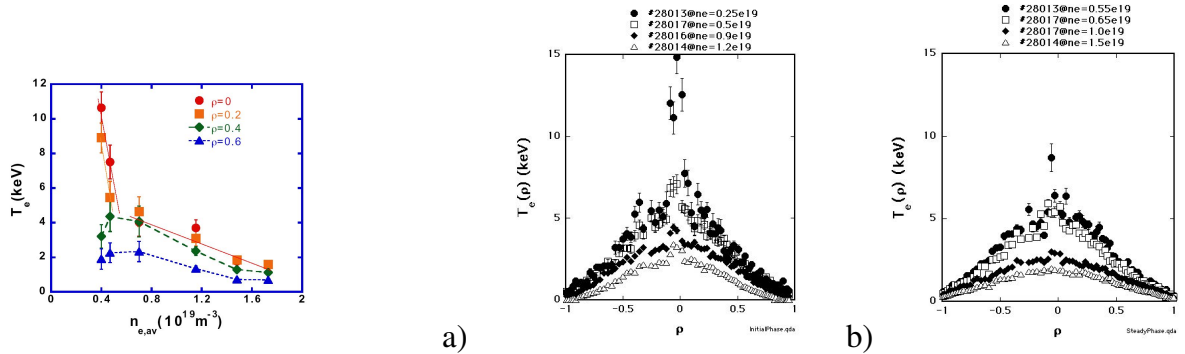


Fig. 4: Dependence of  $T_e$  at  $\rho = 0, 0.2, 0.4,$  and  $0.6$  on the electron density.

Fig. 5: Electron temperature profiles measured by YAG-Laser Thomson scattering system for various density a) just after power increased and b) 200 ms after.

Figure 4 shows the dependence of the temperatures at  $\rho = 0, 0.2, 0.4,$  and  $0.6$  on the averaged electron density under the same injection condition. Since the expected power deposition and the deposition profiles do not change significantly, the sharp increase in the electron temperatures at  $\rho = 0, 0.2$  suggest the presence of some non-linear mechanism. Especially, in the comparison of the time evolution of the electron temperature profiles for the low and high density case as shown in Fig.5. The electron temperature profile shows ITB like feature even at the initial phase of applying high power with a relatively low temperature even at the density more than  $1 \times 10^{19} \text{m}^{-3}$  as shown in Fig.5 a). The foot point of ITB point within here the sharp reduction of the transport appears and spreads outside as the target electron density decreases. In the

low density case, the ITB like structure may appear just after the power exceeds threshold but soon spreads over  $\rho > 0.2$  where sharpness of the transition between high and low confinement region smeared out resulting in the disappearance of prominent ITB foot point.

### 3. ITB formation on NBI target plasma by ECH

The feet of the ITB are more prominent when the ECH is applied on NBI target plasma.

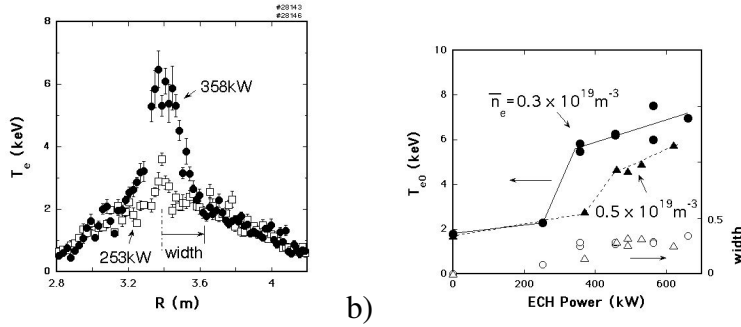


Fig. 6: Typical electron temperature profile during the ITB formation. a)  $T_e$  profile with (triangles) and without (open circles) the ITB for the injection powers of 282 kW and 205 kW, respectively. b) Averaged  $T_{e0}$  as a function of injection power for the averaged electron densities of  $0.3$  and  $0.5 \times 10^{19} \text{ m}^{-3}$ . The dependence of the ITB width as defined in a) is also plotted.

The electron temperature profiles for two different injection powers, one above the threshold (282 kW) and one below it (205 kW), are shown in Fig. 6 a). A high electron temperature gradient is formed with the power above the threshold. The  $\chi_e$  decreases to  $0.7 \text{ m}^2/\text{s}$  from  $2.0 \text{ m}^2/\text{s}$  at the steepest gradient position as the threshold power is exceeded. The dependences of the central electron temperature on the injection power are shown for averaged electron densities of  $0.3$  and  $0.5 \times 10^{19} \text{ m}^{-3}$  in Fig. 6 b). It is clear that the threshold power depends on the electron density. Other observations with respect to the ITB are: 1) The power deposition profile plays an important role in the formation of the ITB. The total deposited power inside  $\rho < 0.2$  seems the key factor. 2) Reduction of the ion and impurity transport is in the ITB are suggested from impurity observations. formation indicates the presence of a positive electric field. 3) The location of the feet of the ITB depends on the direction of the NBI, which may be related to the position of the rational surface  $\iota/2\pi = 0.5$ . 4) The density and electron temperature region of electron root predicted from neoclassical theory coincides with the region where the ITB appears. These facts support the proposed anomalous transport reduction mechanism which the radial electric field shear reduces the fluctuation level and the shear itself is formed by the radial interface between electron and ion root [4]. The  $\iota/2\pi = 0.5$  surface plays an important role in expanding this interface outside. This might be the reason why the width of the ITB foot is rather insensitive to the power, density as shown in Fig. 6 b). The transition between ITB and normal confinement occurred during the turning off and on phase. In Fig. 7 a) and b) shows the response of the electron temperature to the ECH on and off power modulation. These temperatures are measured by multi-channel ECE radiometer. Each line is labelled by measuring position in averaged minor radius. Modulated part of ECH is turned off at  $t = 0.96$  s and on at  $t = 1.06$  s. Another ECH power is applied in the case of Fig. 7 b) to keep the base electron temperature high and to assist the ITB formation. It is clearly seen that the temperature decay in time is much longer in the high temperature case especially in the core region. The changes in the electron density and its profile were negligible. Fast change in the electron temperature just after the turning on and off of the modulated part of ECH reflects the power deposition profile of the modulated power. The power deposition profiles analyzed using just before and after 1.5 ms data at the turn on and off shows in good agreement with that expected from ray tracing calculation [8]. The deduced power deposition profiles are similar in each turn on or off

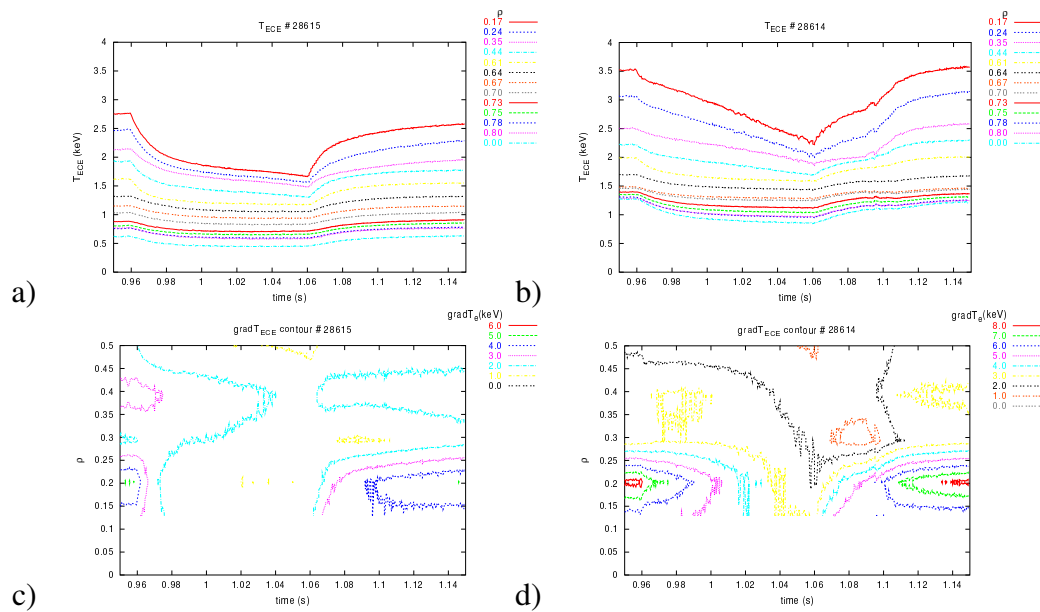


Fig. 7: Time behavior of  $T_e$  measured by ECE. a) without and b) with base ECH on NBI target plasma. c), d) Contour plot of  $\nabla T_e$  estimated from a) and b), respectively

phase for both high and low  $T_e$  cases. Power deposition profile itself is not much affected by the change in the plasma parameters discussed here. Fig. 7 c) and d) show  $\nabla T_e$  contours deduced from difference between adjacent ECE channels shown in Fig. 7 a) and b), respectively. The high normalized gradient  $\frac{\partial T_e}{\partial \rho} > 6$  keV region exists in the high temperature cases and such high gradient states is kept almost 60 ms after the stepwise decrease of the injection power as shown in Fig. 7 d). The high gradient state appears suddenly at 38 ms after the stepwise increase. It is necessary to analyze more in the other plasma parameters and also direct measurement of the radial electric field to draw a conclusion, but these responses support the dynamic model that the suppression of the anomalous transport by the shear in the the radial electric field results in high  $\nabla T_e$  and this high  $\nabla T_e$  lower the threshold level of transition then further expand the transition region [9].

## References

- [1] A. Iiyoshi, M. Fujiwara, O. Motojima et al. Fusion Technol. 17 (1990)169.
- [2] O. Motojima, H. Yamada, A. Komori et al. Phys. Plasmas 6 (1999) 1843.
- [3] K. Itoh, S. -I. Itho, and A. Fukuyama, in *Transport and Structural Formation in Plasmas*, edited by P. Scott and H. Wilhelmsson (Institute of Physics Publishing, Bristol, 1999).
- [4] A. Fujisawa, H. Iguchi, T. Minami, et al. Phys. Plasmas 7 (2000) 4152.
- [5] H. Maassberg, C. D. Beidler, U. Gasparino, et al. Phys. Plasmas 7 (2000) 575.
- [6] C. Alejandre, L. Almuquera, J. Alonso, et al. Nucl. Fusion 41 (2001) 1449.
- [7] S. Kubo, T. Shimozuma, H. Idei, Y. Yoshimura, et al. J. Plasma Fusion Res. 78 (2002) 99.
- [8] S. Kubo, H. Idei, T. Notake, et al. to be published J. Plasma Fusion Res.
- [9] M. Yokoyama, K. Ida, H. Sanuki, et al. Nucl. Fusion 42 (2002) 143.